Cost-effective method of manufacturing a 3D MEMS optical switch

Emily Carr, Ping Zhang, Doug Keebaugh, Kelvin Chau
Glimmerglass Networks, 26142 Eden Landing Rd, Hayward, CA 94545

ABSTRACT

The demand for micro-electro-mechanical system (MEMS) optical switches has been steadily increased due to the rapid growth of data and video transport networks. All-optical switching eliminates the need for optical-electrical conversion offering the ability to switch optical signals transparently: independent of data rates, formats and wavelength. It also provides network operators much needed automation capabilities to create, monitor and protect optical light paths. To further accelerate the market penetration, it is necessary to identify a path to reduce the manufacturing cost significantly as well as enhance the overall system performance, uniformity and reliability. Currently, most MEMS optical switches are assembled through die level flip-chip bonding with either epoxies or solder bumps. This is due to the alignment accuracy requirements of the switch assembly, defect matching of individual die, and cost of the individual components. In this paper, a wafer level assembly approach is reported based on silicon fusion bonding which aims to reduce the packaging time, defect count and cost through volume production. This approach is successfully demonstrated by the integration of two 6-inch wafers: a mirror array wafer and a "snap-guard" wafer, which provides a mechanical structure on top of the micromirror to prevent electrostatic snap-down. The direct silicon-to-silicon bond eliminates the CTE-mismatch and stress issues caused by non-silicon bonding agents. Results from a completed integrated switch assembly will be presented, which demonstrates the reliability and uniformity of some key parameters of this MEMS optical switch.

Keywords: Optical switching, photonic switch, Optical Cross-Connect (OXC), MEMS, MOEMS, fusion bonding, electrostatic operation

1. INTRODUCTION

MEMS optical switch systems based on beam steering mirrors have been explored by many researchers[1-5]. These switches allow many optical channels to be switched in a relatively small amount of space, utilizing micromirrors to switch or reflect an optical signal from one fiber to another dependent on the relative angle of the micromirror, as shown in Fig. 1.

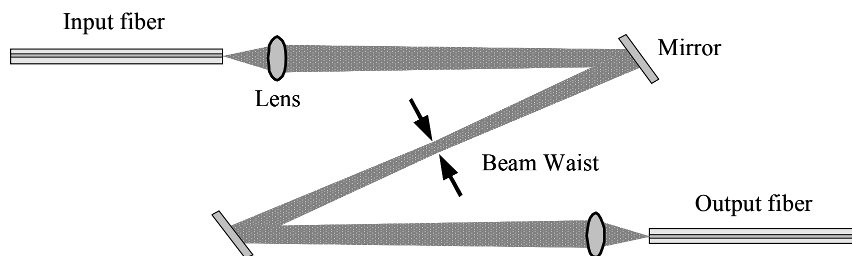

Fig. 1 Simple fiber-to-fiber relay system[5].

The demand for such micro-electro-mechanical system (MEMS) optical switches has been steadily increased due to the many benefits[6] for all-optical applications and the proliferation of fiber optic technology into various markets[7-10]. The use of fiber optics to relay signals over long distances is widespread. Communications, computing, and fiber sensing

Micromachining and Microfabrication Process Technology XIV, edited by Mary-Ann Maher,
Jung-Chih Chiao, Paul J. Resnick, Proceedings of SPIE Vol. 7204, 720402 · © 2009 SPIE
CCC code: 0277-786X/09/$18 · doi: 10.1117/12.810065

systems need to route and switch data signals between specified destinations. MEMS optical switches serve a central function in all of these fiber networks. All-optical switching eliminates the need for optical-electrical conversion, offering the ability to switch optical signals transparently: independent of data rates, formats, wavelengths and protocols as well as services. It has already been utilized to create, monitor and protect optical light paths in various industries. Examples of current roles of optical switching include the management of secure physical layer networks for national security, sensor monitoring for transportation infrastructure, automation of telecommunication central office and equipment protection in Internet peering exchanges. As a basic building block for many optical fiber applications, the MEMS optical switch opens up significant market opportunities.

As carriers continue to deploy Fiber to the X (FTTX) technologies and extend the reach of their optical infrastructure, they encounter the challenge of managing literally thousands of fiber interfaces in a single location. These interfaces are typically managed manually via a bulky patch panel or optical distribution frame (ODF). This manual work is costly, labor-intensive and increases opportunities for human errors. Features of interest now include automatic provisioning, remote configurability and reduced power and space. MEMS optical switches provide operators much needed automation capabilities to create, monitor and protect optical light paths, with reduced provisioning intervals and lower capital and operational costs.

With the tremendous growth in wireless communications, Radio-over-fiber (RoF) technology has attracted much interest from many wireless/RF (radio frequency) applications, i.e., wireless LAN (WLAN) and digital TV transmission systems, which offers high-quality, low-distortion and point-to-point links. There are demands for cost effective RoF switches to enable networks providing features such as link reusability, bandwidth sharing and information broadcast/multicast. Traditional RF switches can only handle small portions of the total frequency band, suffer from much greater levels of Electromagnetic Interference (EMI) from neighboring signals, and have greater signal loss and cost. Optical switches can work across an extremely broad frequency range, thus one optical switch is sufficient to handle HF, UHF, VHF and even microwave frequencies with no EMI and better signal quality. The low loss nature of fiber also allows antennas to be located much longer distances from receivers, with great reductions in size, weight and cost when compared to distribution copper cabling.

The market for fiber sensors is also growing. Fiber optic sensors have many applications in automated factories, mines, offshore platforms, air, sea, land, and space vehicles, energy distribution system and medical patient surveillance systems. Some applications may require very large scale networks with hundreds of sensors. Traditionally, the interrogation system is a major cost burden of a fiber sensor system. By using a time-division multiplexing (TDM) technique, an optical switch could be used to increase the number of sensors as well as reduce the system cost in a fiber sensor network system that minimizes the number of expensive interrogation systems needed for a large array of optical sensors.

Another application is the automation of optical components manufacturing and testing, which is critical to realize cost effective methods to increase the diversity of applications utilizing fiber optic technologies today. Using an optical switch test architecture provides benefits including increased productivity by automation, greater measurement accuracy, removing human errors and lower overall need for test equipment by sharing precious resources, resulting in dramatic cost reductions.

While each unique application may have its own requirements, the core capability of switching light optically in a fiber network remains the same. By employing a MEMS based all-optical switching infrastructure, the cost, performance and reliability can be greatly improved. MEMS optical switches continue to expand into new applications.

2. MOTIVATION

To further accelerate the market penetration, it is necessary to identify a path to reduce the manufacturing cost significantly as well as enhance the overall system performance, uniformity and reliability. Currently, optical MEMS switch modules are assembled through die level flip-chip bonding with either epoxies or solder bumps. To assemble such a multi-chip stack module, the components are fabricated independently at the wafer level, diced, and then assembled though flip-chip bonding[2-5]. The obvious advantages of this assembly approach are to reduce the complexity of manufacturing of each component and optimize the individual fabrication processes to achieve good wafer yield, as

well as being able to match die defects to allow the maximum yield. The trade-offs are that both handling and assembling of discrete components are extremely time consuming and labor intensive.

As the applications and volume of MEMS optical switches increase, it is important to reduce the production time cycle and overall assembly cost. Major economic savings are possible if assembly can be done at the wafer level. Wafer level packaging (WLP)[11] has been adopted in the IC[12] and MEMS[13] industries to meet the market requirements for reduction in both size and cost in recent years. Wafer bonding is a major contributor in reducing the manufacturing costs of the final package. The wafer level capping of fragile microstructures such as accelerometers, gyroscopes and pressure sensors, for protection and sealing purposes is quickly displacing chip-scale packages especially for novel consumer MEMS applications. The development of deep reactive ion etching (DRIE) in combination with wafer bonding also forms a powerful micromachining tool for the fabrication of micromechanical systems[14-15]. With the development of new material and fabrication techniques, as wafer sizes go up, the processing costs per wafer remain about the same, resulting in a decrease in the cost per die.

In this paper, a wafer assembly approach aiming to reduce the cost and improve manufacturability of an optical MEMS switch is presented. The fabrication process and test results of the completed structure are reported as well as discussions on improvements needed to achieve the goal of a cost effective assembly strategy.

3. WAFER BONDING APPROACH

A wafer level bonding approach is investigated, using two optimized 6-inch silicon-on-insulator (SOI) wafers, to create an integrated structure which serves as the key component of our MEMS switch. The cross-section view of one cell of this structure is shown in Fig. 2(b). Traditionally the structures in this assembly are fabricated separately then assembled by flip-chip bonding via epoxy joints (Fig. 2(a)). The top device in the figure, which is an array of patterned through wafer holes, is referred to as the Snap Guard (SG), while the bottom structure is an array of micromirrors, referred to in the figure as MEMS. In the proposed wafer assembly approach, the epoxy will be replaced by a joining feature on the SG as shown in Fig. 2(b), which stands on top of the MEMS chip to form the cavity and enables the direct bonding between the SG chip and the MEMS die at the wafer level. The through-hole SG wafer will be directly bonded to the MEMS wafer using a high-temperature fusion bond technique. One benefit of this technique is that it eliminates the Coefficient of Thermal Expansion (CTE) mismatch between materials with different thermal behavior which could potentially introduce additional stress at the joint surface of the assembly.

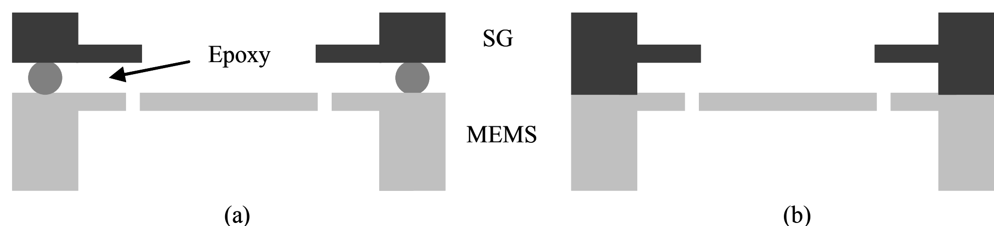

Fig. 2. Cross-section view of the structure assembled by (a) flip-chip bonding and (b) wafer bonding.

There are a number of significant challenges in this wafer level approach. The dimensions of an individual chip on the wafer are approximately 20 mm x 30 mm x 0.5 mm, each consisting of 210 through-holes or mirrors of the size about 1 mm^2. The uniqueness of the geometry and relatively large open areas increase the difficulty of wafer handling during alignment since the processed wafer is held with vacuum in the wafer aligner that is used to perform the aligned wafer bond. In the die-level flip-chip assembly, the gap between the two chips is relatively insignificant and could be compensated by the compliance of the epoxy. In wafer level bonding, it is important to bring the two wafer surfaces in close contact to achieve a strong bond. An appropriate load is also required on the wafers to reduce the wafer bow and form a good bond. The fragility of both the SG and MEMS patterns and small contact area require the wafer bow to be mitigated. Wafer protection during the dicing process and cleaning are also critical in preventing breakage and contamination in this wafer level approach.

4. FABRICATION

The fabrication process flow and a 3-D rendering of fabricated devices are shown in Fig. 3. This process begins with two separately optimized 6-inch SOI wafers. A two-step DRIE process is utilized to create the stand-off and supporting arm on the SG wafer device layer. Followed by the backside etch and removal of the buried oxide, the through-hole structure is constructed. Meanwhile, the mirror wafer is processed independently to form the mirror array pattern. After cleaning, the two wafers are aligned and joined by fusion bonding. The backside cavity is then opened under the mirror.

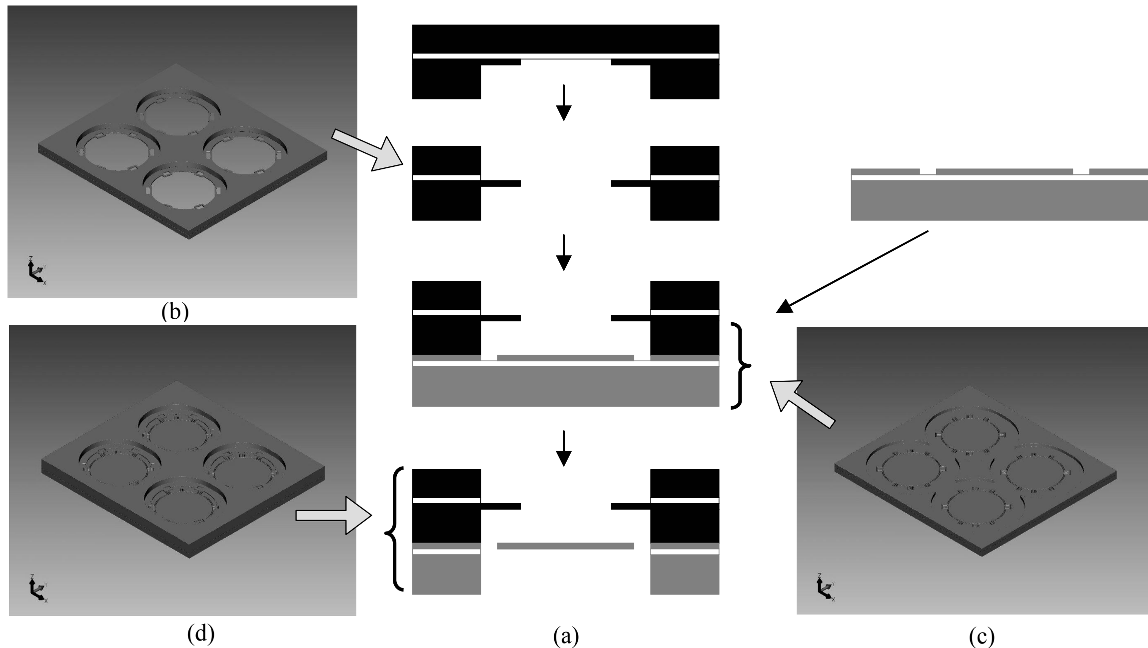

Fig. 3. (a) Fabrication process flow and 3D rendering of fabricated devices. (b) Top view of the snap guard (SG) array, (c) View of MEMS array with the bonding area of the SG wafer shown and (d) Completed assembly.

An infrared (IR) camera was used to investigate the wafer bonding quality. The IR images of the bonded wafers before and after annealing at 1100°C are shown in Fig. 4. The images reveal the voids (darker areas) between two wafers after initial wafer alignment and heat treatments. Due to wafer bow, the bonding between the two wafers is better in the center than around the edge. This agrees with the observation of voids around the edge shown in Fig. 4(a). After annealing, Fig. 4(b) indicates an increased bonding area with fewer voids in the center and around the edge.

Laser dicing was used to separate the integrated wafers into individual chip stacks. Perforation lines were first created on the wafer surface and then the singulation was accomplished by tape expansion. This approach is ideal for fragile structures since it reduces both the risk of generating particles and mechanical stress compared to the conventional method of using a dicing saw. After cleaning, the chips were metalized on both sides. The integrated structure of the SG and the MEMS is shown in Fig. 5. Metal coating is an important step to the success of fabricating an optical switch. Coating stress could induce an unwanted curvature in individual micromirrors at the temperature range of applications, negatively affecting the optical quality and switch operation. In the flip-chip bonding approach, the metallization process is optimized on the MEMS chip, which is independent of the SG. While in the bonded wafers, the SG structure could create a shadowing effect on the hinges of the MEMS, resulting in a non-uniform metal coating and undesirable mechanical effects that change the functional characteristics of the optical switch.

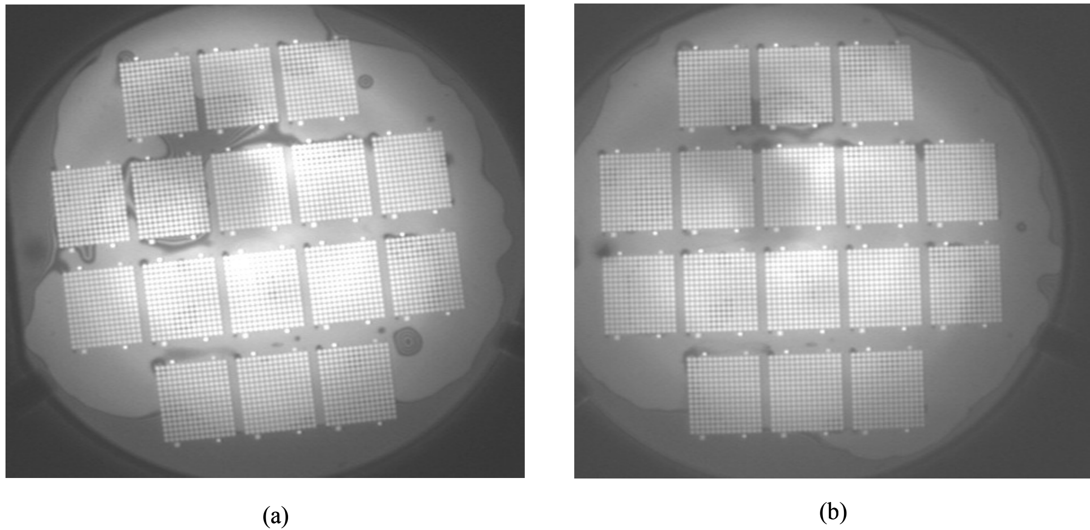

Fig . 4. IR images of the bonded wafers. (a) Before anneal. (b) After anneal.

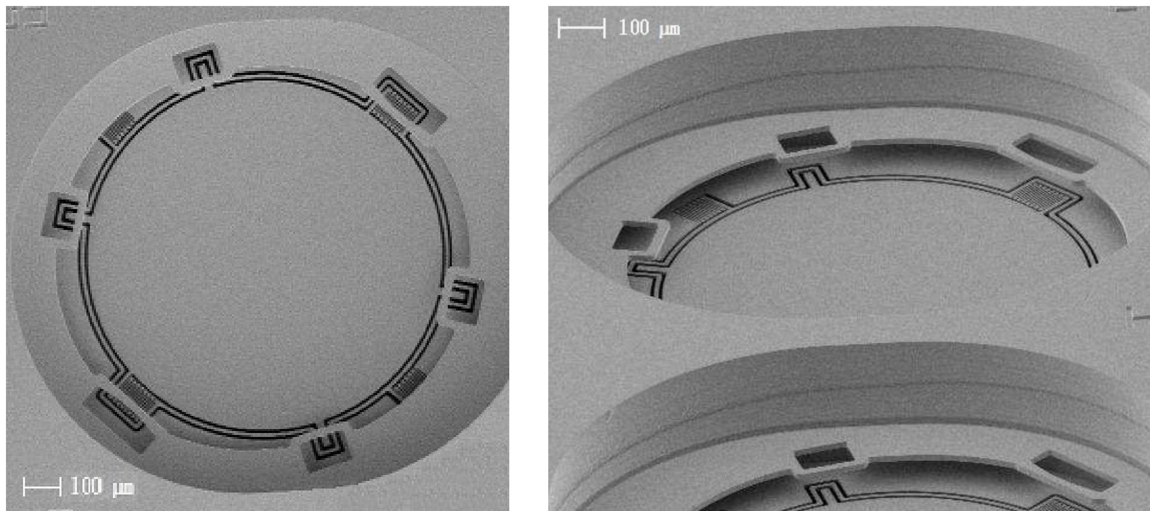

Fig. 5. SEM images of completed integrated snap guard and MEMS assembly from two different angles.

5. TEST RESULTS

The integration of two 6-inch wafers, a mirror array wafer and a "snap-guard" wafer, had been successfully fabricated as shown in Fig. 5. The next step is to verify its functional performance in comparison with the current approach. To complete these tests, an optical switch module was built with this integrated structure, as a complete replacement to the original two parts and then bonded to the electrical structure using the current assembly process[5]. The final structure forms a parallel plate capacitor to which voltages were applied to achieve the mirror tilting and switching requirements. After the optical switch module was created, tests were performed to ensure functionality and uniformity of each MEMS device. A customized test stand was used to measure mirror rotation angles in both axes (up to 10°) with 0.02°of angular displacement resolution. The natural resonance frequencies of each device in both axes were measured as well as operational resonance frequencies under bias. The methodology of these characterizations had been described in previous work[5,16].

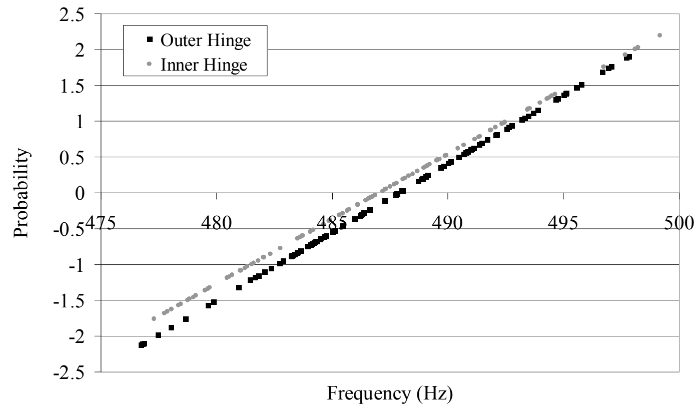

Fig. 6. Natural frequency results of the inner and outer hinges for each device in the array of the integrated device. The vertical axis is in units of standard deviations.

The natural frequencies of two orthogonal sets of mirror hinges were measured. The results of all the mirrors of this module are shown in Fig. 6. The average natural frequency of the inner axis is 487.0 Hz and the outer axis is 487.8 Hz. All of the functional devices of this array fell within the (average $\pm$ 2.5σ) probability range. According to our production experience, the standard deviation shown with this device (inner frequency: σ=5.5 Hz and outer frequency: σ=5.2 Hz) often leads to good performance of the entire module.

The effects of metal coatings on the mechanical properties of the silicon were evaluated with curvature tests and the spectrum analysis. Curvature tests were performed prior to the epoxy bonding steps and then after heat treatment at 120°C. The change in average curvature (1/m) that was observed is consistent with MEMS devices assembled with only flip-chip bonding. By sweeping the frequency of the drive voltage over a selected range, 150 to 1700 Hz, as required by the servo system at higher frequencies, the mechanical spectrum[17] was analyzed and compared to the existing flip-chip design in the mechanical domain. The results from both designs are shown in Fig. 7. Except for a minor shift in resonant frequency, the general characteristics are almost identical. We conclude that the new design does not impact the functional performance. Reflectivity measurements were also performed on the integrated device and were comparable to our flip-chip bonded die. The metal coating process of the integrated die is equivalent to that of our standard flip-chip bonding die and will perform with the same degree of reliability as our current flip-chip bonded assembly.

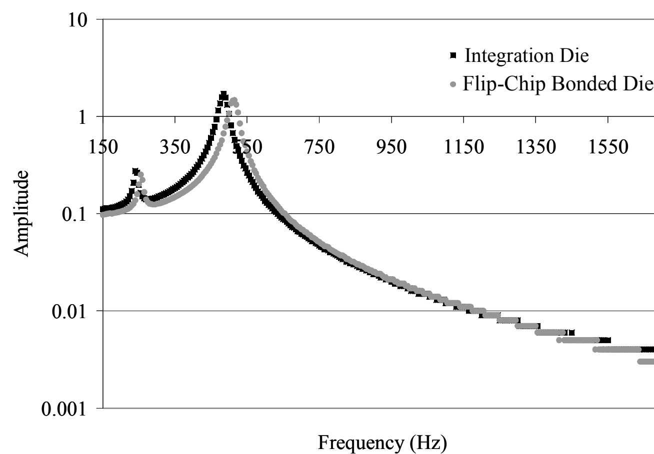

Fig. 7. Inner hinge frequency response of the integration die and a production flip-chip bonded die.

Evaluation of mirror rotation angle is accomplished by tilting the mirrors along a series of radial paths starting in one direction and then increasing until a full 360° had been sampled. An example of the results of this test is shown in Fig. 8. Each path is terminated when the device reaches the maximum tilt, after which the device returns to the 0° tilt state. All of the devices that were tested showed similar characteristics to those shown in Fig. 8.

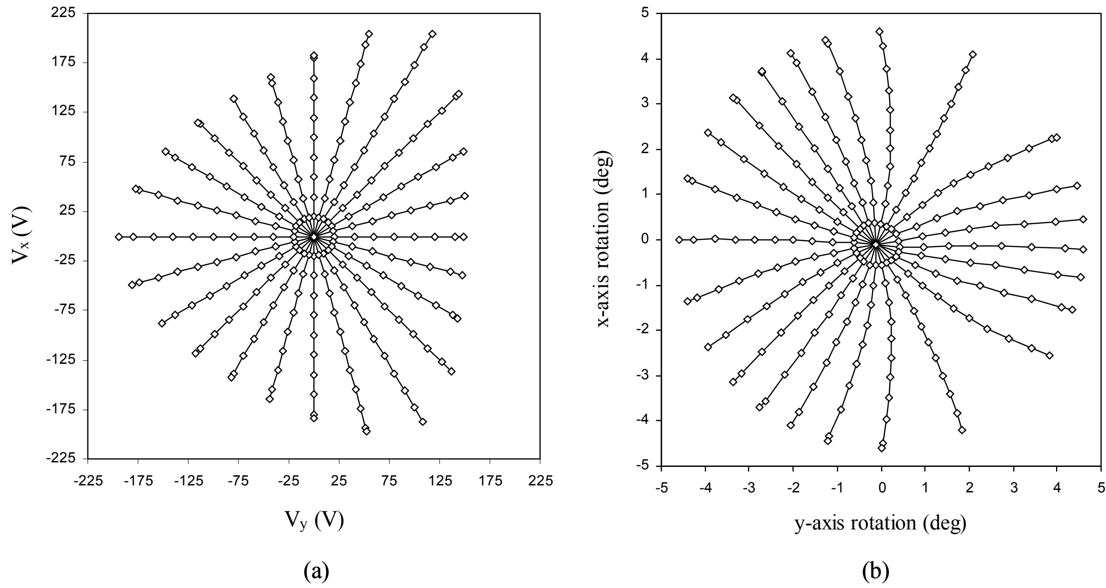

Fig. 8. Measurement of the deflection characteristics of a single mirror in the array. (a) is the series of differential voltage ranges applied to generate deflections. (b) The plot of mirror tilt angle under applied bias along 24 axes.

The operational frequency result is shown in Fig. 9, which is very critical to the control system[16]. The results show that during normal operation the springs suffer from an electrostatic spring softening phenomena as well as an angular dependence to frequency. This result is similar to results obtained with a flip-chip bonded die device with the same natural frequency response.

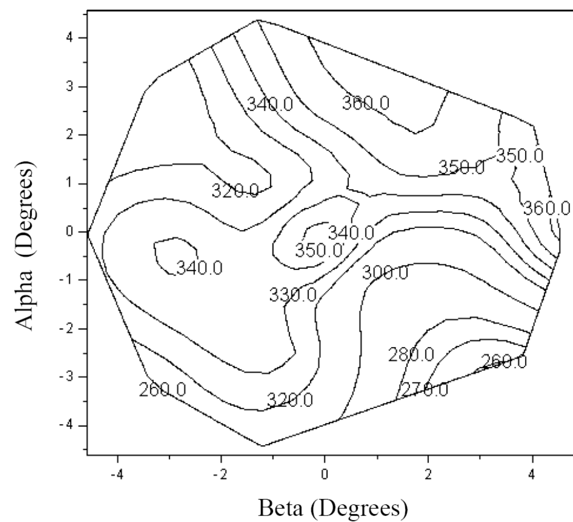

Fig. 9. Operational frequency response (Hz) of a device in the array.

6. CONCLUSION

In summary, a wafer assembly approach of manufacturing a 3-D MEMS optical switch has been investigated. The fabrication process has been successfully demonstrated and module performance has been evaluated. The integrated structure indicates very good uniformity in mechanical and electrical characterizations. The reliability of the alignment of the device is improved at the wafer scale compared to the current flip-chip bonding technique as human error is removed. During fabrication, we noticed that wafer bow is a dominant factor to determine the bonding quality and has a great impact on the final yield. Our future work includes further development in process to overcome wafer bow, improve the yield and study the long term reliability of the integrated device.

ACKNOWLEDGEMENTS

We acknowledge Lihua Li at MEMSCAP, Inc. for the fabrication of the arrays, IR images of the wafers as well as SEM pictures of the completed devices.

REFERENCES

1. D. J. Bishop, C. R. Giles, and G. P. Austin, "The Lucent Lambda router: MEMS Technology of the Future Here Today," *IEEE Communications Magazine*, vol. 40, pp. 75-79, 2003.
2. A. Kazama, M. Horino, K. Fukuda, M. Kanamaru, T. Akashi, T. Ishikawa, T. Harada and R. Okada, "Low-insertion-loss compact 3D-MEMS optical matrix switch with 18 input/output ports," *Tech Dig Sens Sym*, vol. 21, pp. 323-328, 2004.
3. J. Yamaguchi, T. Sakata, N. Shimoyama, H. Ishii, F. Shimokawa, and T. Yamamoto, "High-yield Fabrication Methods for MEMS Tilt Mirror Array for Optical Switches," *NTT Technical Review*, vol. 5, No. 10, pp. 1-6, 2007.
4. T. Yamamoto *et al.*, "A three-dimensional MEMS optical switching module having 100 input and 100 output ports," *IEEE Photon. Technol. Lett.*, vol. 15, No. 10, pp. 1360–1362, Oct. 2003.
5. A. Fernandez, B. P. Staker, W. E. Owens, L. P. Muray, J. P. Spallas and W. C. Banyai, "Modular MEMS Design and Fabrication for an 80 x 80 Transparent Optical Cross-Connect Switch," *Proc. of SPIE*, vol. 5604, pp. 208-217, 2004.
6. Y. Su, H. Peng and Y. Li, "The application and analysis of MEMS optical switches," *Proc. of SPIE*, vol. 6021, pp. 780-789, 2005.
7. K. C. Nguyen, "Three-dimensional MEMS optical switch for fiber optic communication applications," *Proc. Of SPIE*, vol. 4907, pp. 31-35, 2002.
8. B. Mead, "Optical Switches Link Multiple Receivers to Remote Antennas", *Microwave & RF*, Aug 2006.
9. M. Fabbri and P. Faccin, "Radio over Fiber Technologies and Systems: New Opportunities," *ICTON 2007 Conf*, vol. 3, pp. 230 – 233, 2007.
10. M. J. Bitting, "Optical switching for automated test systems", *IEEE AUTOTESTCON Proceedings*, pp 140-151, 2002.
11. P. Garrou, D.C. Co and R.T. Park "Wafer Level Chip Scale Packaging (WL-CSP): An Overview, " *IEEE Trans on Advanced Packaging*, vol. 23, No. 2, pp. 198-205, May 2000.
12. G. Carchon, W. De Raedt, and E. Beyne, "Wafer-level packaging technology for High-Q On-chip Inductors and Transmission Lines, " *IEEE Trans. MTT*, vol. 52, no.4, pp. 1244 – 1251, April 2004.
13. A.R Mirza, "Wafer-level packaging technology for MEMS, " *IEEE ITHERM 2000 Conf*, vol. 1, 119, 2000.
14. C. Harendt, H-G. Graf, B. Hoemnger and E. Penteker, "Silicon fusion bonding and its characterization," *J. Micromech. Microeng*., vol. 2, pp. 113-116, 1992.
15. E. H. Klaassen, K. Petersen, J. M. Noworolski, J. Logan, N. I. Maluf, J. Brown, C. Storment, W. McCulley, and G. T. A. Kovacs, "Silicon fusion bonding and deep reactive ion etching: a new technology for microstructures," *Sensors and Actuators A (Physical),* vol. 52, no.1-3, pp. 132-139, 1996.
16. W. C. Dickson, B. P. Staker, G. Campbell, and W. C. Banyai, "64x64 3D-MEMS switch control system with robustness to MEMS resonant frequency variation and pointing drift, " *OFC2004 Technical Digest*, ThQ5, 2004.
17. L. A. Rocha, E. Cretu, G. de Graaf, R. F. Wolffenbuttel, "Mechanical spectrum analyzer in silicon using micromachined accelerometers with time-varying electrostatic feedback," *Proc. IMTC2003, the 20th IEEE Intrum. Meas. Techn. Conf.*, pp. 1197-1201, 2003.